ISSN 1063-7834, Physics of the Solid State, 2016, Vol. 58, No. 4, pp. 743–747. © Pleiades Publishing, Ltd., 2016.
Original Russian Text © O.A. Kogtenkova, A.B. Straumal, N.S. Afonikova, A.A. Mazilkin, K.I. Kolesnikova, B.B. Straumal, 2016, published in Fizika Tverdogo Tela, 2016, Vol. 58, No. 4, pp. 721–724.

PHASE TRANSITIONS

Grain Boundary Wetting Phase Transitions in Peritectic Copper—Cobalt Alloys

O. A. Kogtenkova[a]*, A. B. Straumal[a, b], N. S. Afonikova[a], A. A. Mazilkin[a], K. I. Kolesnikova[a], and B. B. Straumal[a, b]

[a] *Solid State Physics Institute, Russian Academy of Sciences, Institutskaya ul. 2, Chernogolovka, Moscow oblast, 142432 Russia*

[b] *National University of Science and Technology "MISIS", Leninskii pr. 4, Moscow, 119049 Russia*

* *e-mail: koololga@issp.ac.ru*

Received July 23, 2015

Abstract—The transition from incomplete to complete grain boundary wetting in copper alloys with 2.2 and 4.9 wt % Co is studied. These alloys with peritectic phase diagrams differ from previously studied systems with eutectic transformation by the fact that the melt layer separating grains from each other is not enriched, but is depleted by the second component (cobalt in this case). The fraction of completely wetted grain boundaries increases with temperature, as in eutectic systems, from zero at a temperature of 1098°C to ~80% at 1096°C. For symmetric twin boundaries, the temperature dependence of the contact angle with melt drops is constructed. As in the eutectic systems, the contact angle decreases with increasing temperature (although not to zero due to the extremely low energy of symmetric twin boundaries).

DOI: 10.1134/S1063783416040107

1. INTRODUCTION

Alloys of the Cu–Co peritectic system [1, 2] attract the interest of researchers due to their magnetic properties (giant magnetoresistance [3]), their applicability as catalysts in synthesis of higher alcohols [4], and extraordinary mechanical properties [5]. Therefore, in recent years, the Cu–Co phase diagram has been extensively studied and improved (see [6, 7] and references therein). The high positive enthalpy of copper and cobalt mixing leads to some interesting phenomena, e.g., the existence of the metastable solubility limit in the supercooled melt region (see [8, 9] and references therein]. There the so-called grain-boundary (GB) phase transformations are observed, in particular, wetting phase transitions at grain boundaries (GBs) [10–12]. Recently, such phenomena were also observed in cobalt-based alloys [13]. Nevertheless, GB wetting transitions have not been studied in peritectic systems. From this point of view, Cu–Co alloys in the high-cooper concentration region are very attractive and promising.

GB phase transformations can change significantly polycrystal properties [10, 14]. The most important GB phase transformation is the transition from incomplete grain boundary wetting of the second phase to the complete one [10]. The wetting phase can be either liquid or solid [12, 15]. In the case of incomplete wetting, the contact angle between the second phase and GB is nonzero, $\theta > 0°C$, and the wetting phase forms lenticular particles separated by "dry" GB regions. The reason is that that the GB enthalpy per σ_{GB} unit area was lower than the GB enthalpy of two phase interfaces σ_{GB} ($\sigma_{GB} > 2\sigma_{IB}$). In the case of complete wetting, $\sigma_{GB} > 2\sigma_{IB}$, $\theta = 0°C$, and the wetting phase layer completely substitutes GB. The transition from incomplete to complete GB wetting by liquid phase (melt) at a certain temperature T_w is described by a horizontal tie-line in the two-phase "solid solution + liquid" region of the bulk phase diagram [11, 12]. Such a tie-line connects points on solidus and liquidus curves at the temperature T_w. These grain-boundary wetting phenomena were studied for a wide range of systems on both polycrystals [11, 12, 16] and single GBs in specially grown bicrystals [11, 15].

The creep behavior of polycrystalline solid solutions of cobalt in copper and their surface tension were recently studied under the solidus curve of the Cu–Co phase diagram [17, 18]. The creep activation enthalpy of pure copper was close to the activation enthalpy of bulk self-diffusion of copper. The creep activation enthalpy of Cu–Co solid solutions was lower than that of pure copper in all cases. Furthermore, experimental points for the Cu–Co solid solution viscosity in the Arrhenius coordinates can be approximated by two straight lines with a discontinuity at a certain temperature. Such creep behavior of Cu–Co solid solutions is

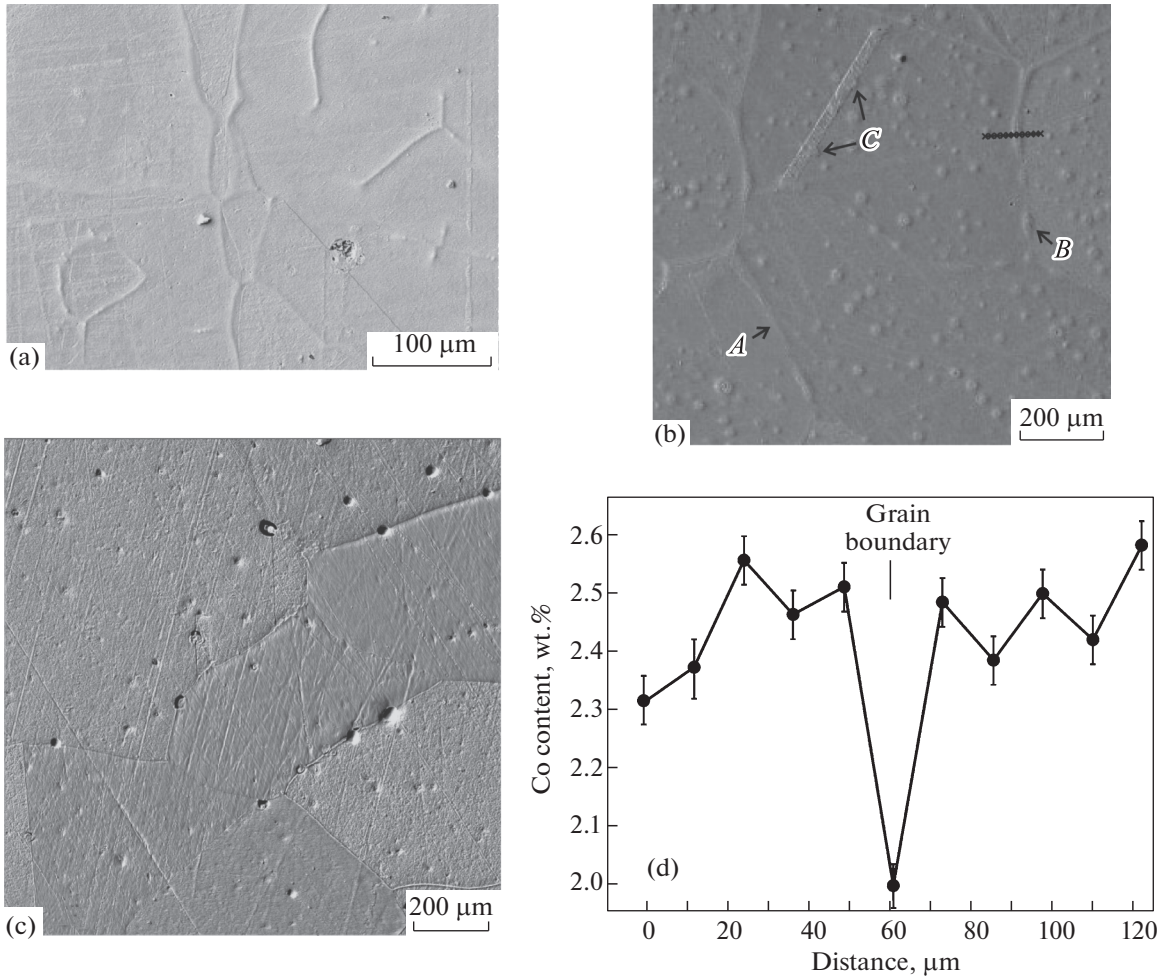

Fig. 1. SEM micrographs of the Cu alloy with 2.2 wt % Co, annealed at (a) 1096°C, (b) 1092°C, and (c) 1086°C. (d) Concentration profile of the Co distribution in the direction perpendicular to the grain boundary (straight line segment with experimental points in Fig. 1b).

explained by changes in GB properties in coarse-grained polycrystals under study [17, 18].

The objective of this work is to study the structure and properties of grain boundaries formed due to wetting phase transitions in polycrystals in the Cu–Co system.

2. EXPERIMENTAL TECHNIQUE

Copper alloys with 2.2 and 4.9 wt % Co were produced as cylindrical ingots 10 mm in diameter by vacuum induction melting using high-purity-grade components (5*N* Cu, 5*N* Co). For further studies, disks 0.4 mm thick were cut off from ingots using spark cutting. After chemical etching, these disks were sealed in quartz cells with a residual pressure of 4×10^{-4} Pa for subsequent annealings in a temperature range from 1084 to 1096°C (the annealing temperature control accuracy was ±1°C). After annealings, water quenching was performed.

For metallographic studies, the samples were ground by sandpaper, polished by diamond paste with a granularity of 6, 3, and 1 μm, and were etched for 5–10 s in an $H_2O + HNO_3$ solution with a volume concentration ratio of 1 : 1. The optical microscopy study was performed using a Neophot-32 microscope. The scanning electron microscopy (SEM) study was performed using a Philips XL30 scanning microscopy with a LINK ISIS energy-dispersive spectrometer (Oxford Instruments).

3. RESULTS AND DISCUSSION

In the Cu–Co peritectic system, complete and incomplete grain-boundary wetting was observed for the first time, when the wetting layer on the GB is depleted by the second component, rather than enriched, as in the case of alloys with eutectic transformations [10–12, 16]. Figure 1 shows the effect of the grain-boundary wetting phase transition on the

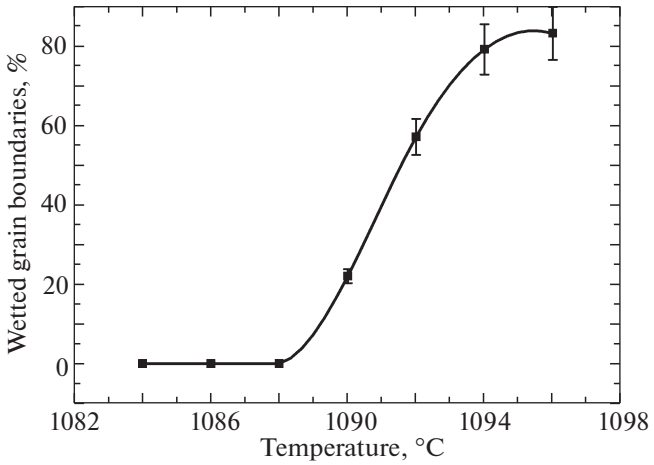

Fig. 2. Temperature dependence of the fraction of completely wetted grain boundaries in the Cu alloy with 2.2 wt % Co.

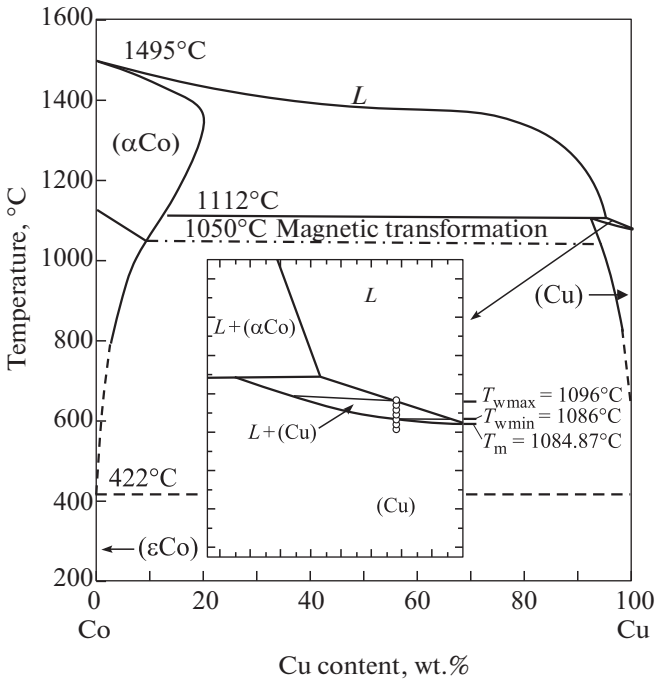

Fig. 3. Phase diagram of the Cu–Co system with lines of volume phase transitions [20] and wetting phase transition tie-lines at $T_{w\,max}$ = 1096°C and $T_{w\,min}$ = 1086°C. In the inset, circles are experimental points, T_m is the copper melting temperature.

microstructure of polycrystals in the two-phase region L + (αCu) in the Cu alloy with 2.2 wt % Co. The microstructure of all annealed samples represents solid solution (Cu) grains; symmetric twin boundaries (some of them are faceted [19]) are arranged mostly along sample edges; in the bulk, there are the second phase segregations, i.e., the copper solid solution in cobalt (Co) at grain boundaries (Cu)/(Cu) and at symmetric twin boundaries. The second phase (Co) precipitations are arranged uniformly over the grain volume (they are spherical there) and over GBs. At the bulk solidus temperature T = 1097°C [20], their size is 20–30 μm; at the bulk solvus temperature T = 1091°C [20], their size decreases approximately twice.

We can see that almost all grain boundaries (~80%) in the alloy are coated with a thin melt layer at the annealing temperature 1096°C (Fig. 1a). At a temperature of 1094°C (Fig. 1b), the number of completely wetted boundaries is significantly smaller, whereas no completely wetted boundaries are observed at a temperature of 1086°C (Fig. 1c). Figure 1b shows the completely wetted (indicated by symbol *A*) and partially wetted (indicated by symbol *B*) GBs and the symmetric twin boundary (indicated by symbol *C*) with the second phase segregations over the boundary. Figure 1d shows the concentration profile of the cobalt distribution perpendicular to grain boundaries (straight line segment with experimental points in Fig. 1b). In this portion, a minimum cobalt concentration corresponds to the grain boundary (Cu)/(Cu) position. As noted above, this is associated with the peritectic transformation in this diagram region, and wetting phase (melt) contains a smaller cobalt content than the copper-based solid solution.

The temperature dependence of the fraction of completely wetted boundaries is shown in Fig. 2. An increase in the fraction of completely wetted boundaries (from 0 to 80%) is observed in the temperature range from 1086 to 1096°C. Thus, the wetting phase transition in the Cu–Co system occurs in the temperature range from 1086 to 1096°C. The differences in the temperatures of the transition from incomplete to complete wetting are associated with the differences in grain boundary σ_{GB} and interphase boundary σ_{IB} energies, which are controlled by the misorientation angle [10, 22]. Using the data obtained, tie-lines of the wetting phase transition at $T_{w\,max}$ = 1096°C and $T_{w\,min}$ = 1086°C were constructed (solid thin curves in the region L + (Cu)) in the bulk Cu–Co phase diagram (Fig. 3).

In this study, we showed that the second phase particle in the obtained structures are formed not only in the bulk and over GBs, but also at symmetric twin boundaries (in Fig. 1b, they are indicated by symbol *C*). The samples under study are polycrystals in which grains are randomly oriented. Therefore, GBs in a material have different energies [22]. This is also supported by and the difference in the temperatures of the transitions from incomplete to complete wetting (Figs. 2 and 3) [10]. Twin boundaries have the advantage that they can be easily identified without a local orientation analysis using backscattered electron diffraction. The point is that symmetric twin boundaries form characteristic pairs, i.e., so-called twin plates (see Fig. 1b, indicated by symbol *C*) [19]. A facet of the

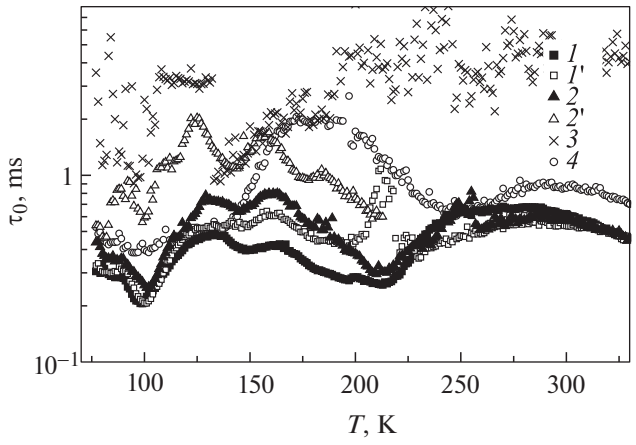

Fig. 4. Temperature dependence of the contact angle between particles (Co) and symmetric twin boundaries.

asymmetric twin boundary (the so-called 9*R* facet [19]) is on the edge of such plates. Symmetric twin boundaries can also be easily found in all annealed samples under study. This allowed measurements on polycrystals, for which bicrystals with single boundaries should be usually grown [10, 16]. Figure 4 shows the temperature dependence of the contact angle θ between particles (Co) and symmetric twin boundaries. As the temperature increases, the contact angle θ decreases from 106 to 58°C. In other words, although the contact angle at symmetric twin boundaries decreases with increasing temperature, it does not reach zero. This is explained by the circumstance that symmetric twin boundaries have an extremely low energy σ_{GB} [19].

Previously, it was found that if the second phase wetting grain boundaries is solid, rather than liquid, the fraction of wetted boundaries can increase with decreasing, rather than increasing temperature [21, 23]. Accordingly, the contact angle decreases with decreasing, rather than increasing temperature. This is because the energy of interphase boundaries (if the second phase is solid) can decrease with increasing temperature more slowly, than the grain boundary energy. It was a priori unclear whether a similar phenomenon will be observed in the case where we deal with a liquid wetting phase which is not enriched, but is depleted by the second component. We saw that, at least in the case of copper–cobalt alloys, this is not observed, and the fraction of completely wetted boundaries and the contact angle behave similarly as for the melt enriched by the second component.

4. CONCLUSIONS

The transition from incomplete to complete wetting of grain boundaries in alloys with peritectic phase diagrams was studied for the first time by the example of the copper–cobalt system. These alloys differ from previously studied systems with eutectic transformation by the fact that the melt layer separating grains from each other is not enriched, but is depleted by the second component (cobalt in the case at hand). The fraction of completely wetted boundaries increases with temperature, as in eutectic systems, from zero at a temperature of 1086°C to approximately 80% at 1096°C. The fraction of 20% of the boundaries remained incompletely wetted includes both symmetric twin boundaries and others GBs with low energies, most likely, low-angle boundaries. Since all studied samples contained symmetric twin boundaries, we were able to construct the temperature dependence of the contact angle with melt drops for them. As in eutectic systems, the contact angle decreases with increasing temperature (although not to zero due to the extremely low energy of symmetric twin boundaries).

ACKNOWLEDGMENTS

This study was supported by the Russian Foundation for Basic Research, project no. 14-08-00972.

REFERENCES

1. T. Nishizawa and K. Ishida, Bull. Alloy Phase Diagrams **5**, 161 (1984).
2. Y. Nakagawa, Acta Metall. **6**, 704 (1958).
3. G. Binasch, P. Grünberg, F. Saurenbach, and W. Zinn, Phys. Rev. B: Condens. Matter **39**, 4828 (1989).
4. J. P. Hindermann, G. J. Hutchings, and A. Kiennemann, Catal. Rev. **35**, 1 (1993).
5. B. B. Straumal, A. A. Mazilkin, B. Baretzky, E. Rabkin, and R. Z. Valiev, Mater. Trans. **53**, 63 (2012).
6. M. A. Turchanin and P. G. Agraval, Powder Metall. Met. Ceram. **46**, 77 (2007).
7. M. Palumbo, S. Curiotto, and L. Battezzati, CALPHAD: Comput. Coupling Phase Diagrams Thermochem. **30**, 171 (2006).
8. B. Schwarz, N. Mattern, O. Shuleshova, and J. Eckert, Intermetallics **32**, 250 (2013).
9. S. Curiotto, R. Greco, N. H. Pryds, E. Johnson, and L. Battezzati, Fluid Phase Equilib. **256**, 132 (2007).
10. B. B. Straumal, W. Gust, and D. A. Molodov, Interface Sci. **3**, 127 (1995).
11. B. Straumal and W. Gust, Mater. Sci. Forum **207**, 59 (1996).
12. B. Straumal, W. Gust, and T. Watanabe, Mater. Sci. Forum **294**, 411 (1999).
13. S. Curiotto and D. Chatain, Scr. Mater. **60**, 40 (2009).
14. T. R. Bieler, R. Barabash, D. Spearot, J. Luo, and S. Dillon, Metall. Mater. Trans A **43**, 3515 (2012).
15. V. N. Semenov, B. B. Straumal, V. G. Glebovsky, and W. Gust, J. Cryst. Growth **151**, 180 (1995).

16. B. B. Straumal, B. Baretzky, O. A. Kogtenkova, A. B. Straumal, and A. S. Sidorenko, J. Mater. Sci. **45**, 2057 (2010).
17. S. N. Zhevnenko and E. I. Gershman, J. Alloys Compd. **536**, S554 (2012).
18. S. N. Zhevnenko, Metall. Mater. Trans. A **44**, 2533 (2013).
19. B. B. Straumal, S. A. Polyakov, and E. J. Mittemeijer, Acta Mater. **54**, 167 (2006).
20. *Binary Alloy Phase Diagrams*, Ed. by T. B. Massalski, 2nd ed. (ASM International, Materials Park, Ohio, United States, 1990).
21. B. Straumal, R. Valiev, O. Kogtenkova, P. Zieba, T. Czeppe, E. Bielanska, and M. Faryna, Acta Mater. **56**, 6123 (2008).
22. B. B. Straumal, L. M. Klinger, and L. S. Shvindlerman, Acta Metall. **32**, 1355 (1984).
23. B. B. Straumal, O. A. Kogtenkova, A. B. Straumal, Yu. O. Kuchyeyev, and B. Baretzky, J. Mater. Sci. **45**, 4271 (2010).

Translated by A. Kazantsev

SPELL: 1. solvus